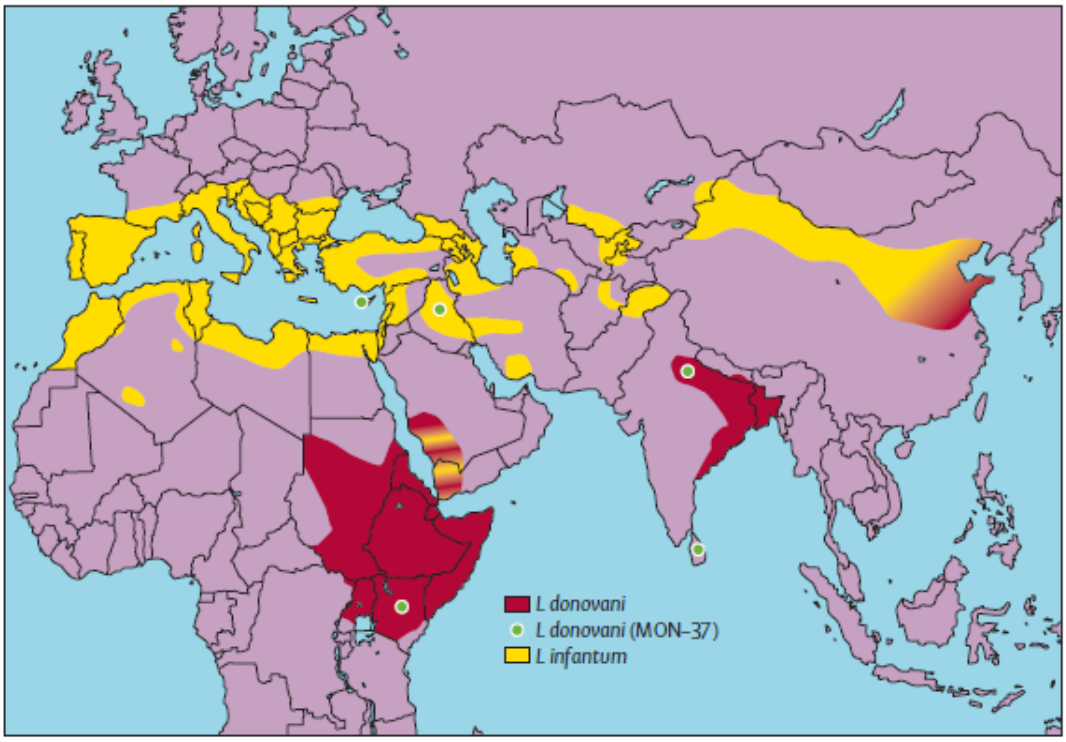

Figure: Distribution of *Leishmania donovani* complex species in the Old World and localisation of the MON-37

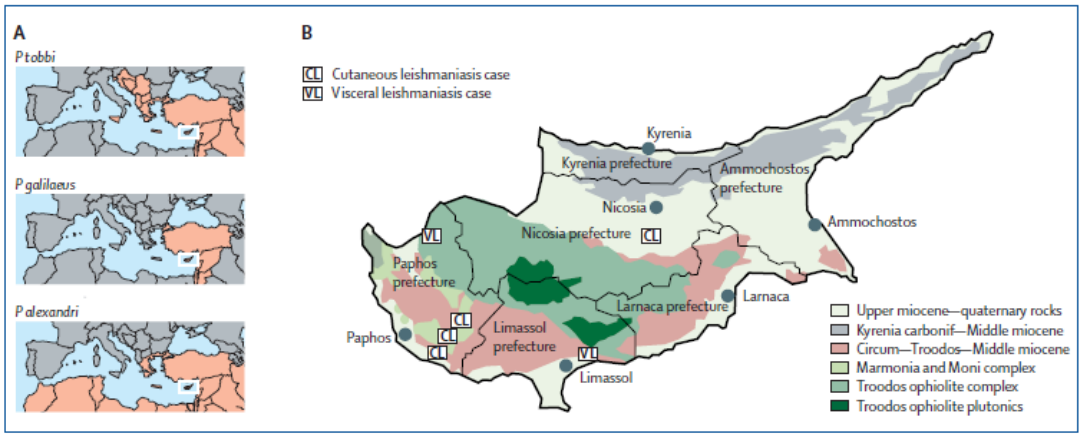

Figure: Regional distribution of three putative *Phlebotomus* spp vectors (A) and locations of the human *L donovani* cases in Cyprus (B)

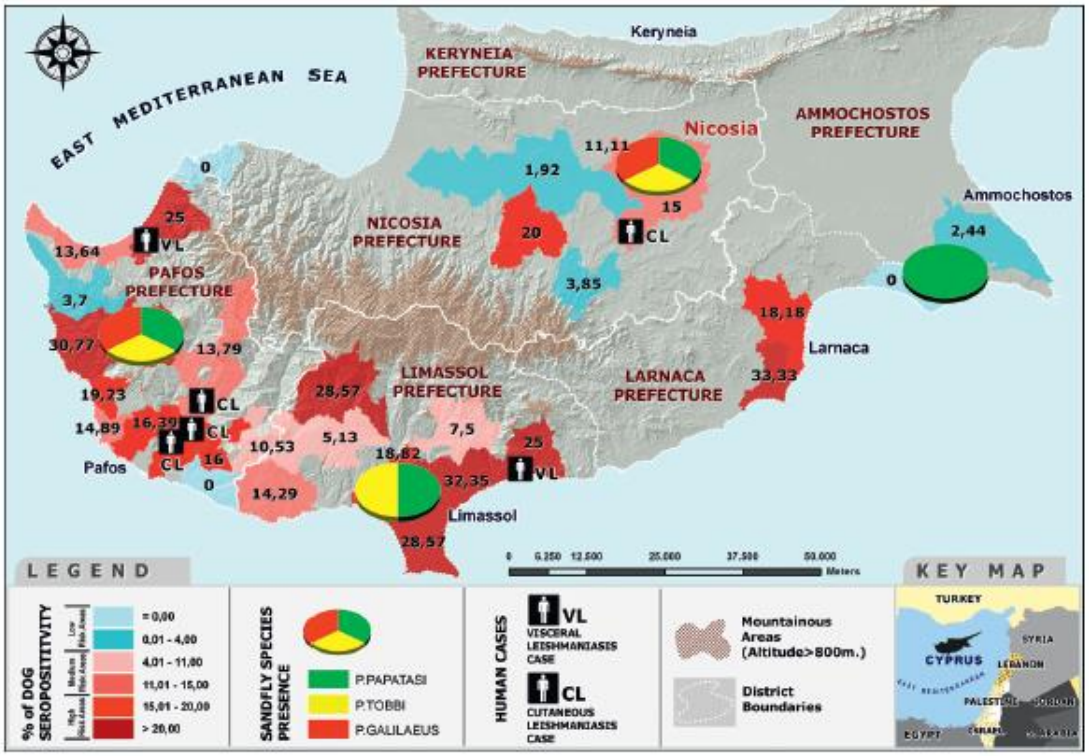

FIGURE 1. Map of Cyprus showing dog seropositivity (%) caused by *L. infantum* in the 30 squares studied (the boundaries of the selected villages in each square are shown). CL and VL, both caused by *L. donovani* MON-37, and the presence of the main *Phlebotomus* spp. caught in the four prefectures are shown.

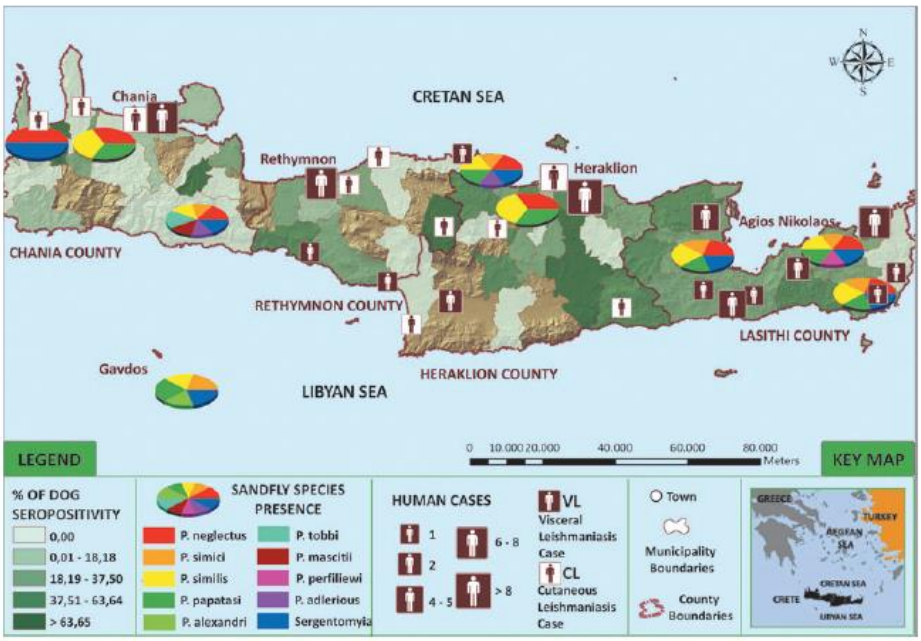

FIG. 1. Geographical distribution of human leishmaniases cases (VL, visceral; CL, cutaneous) in Crete, in relation to *Phlebotomus* species presence and dog seropositivity. (*P. adlerious* is now Alderius subgenus.)

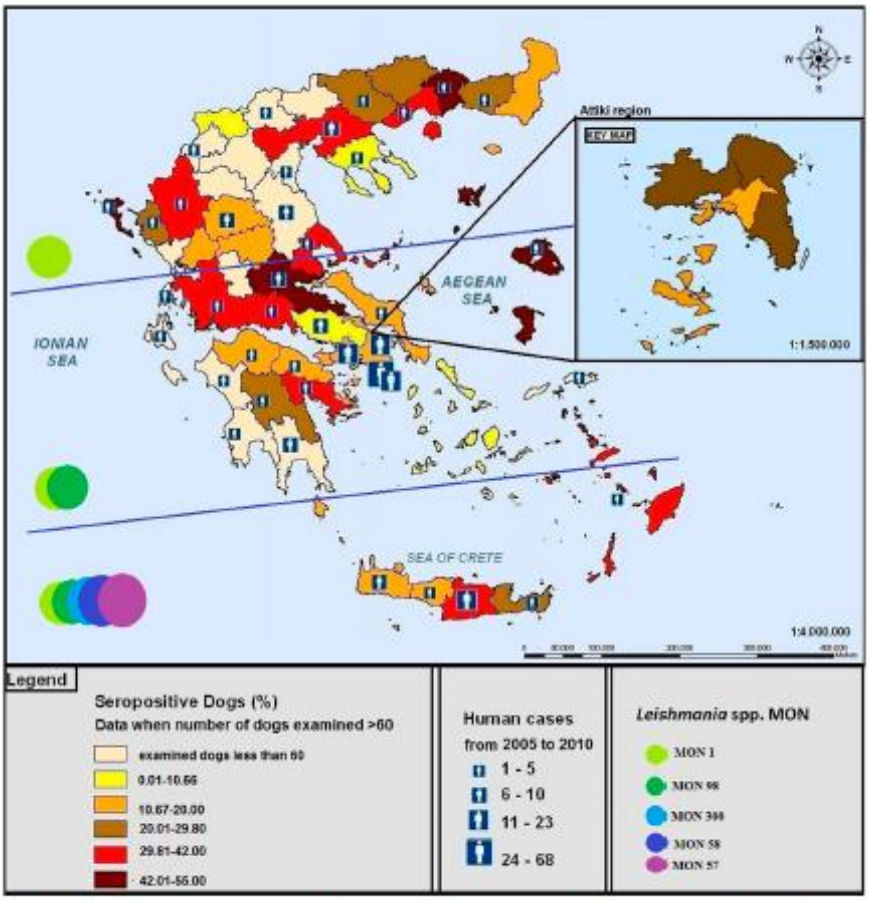

FIGURE 2. Geographical distribution of human leishmaniasis cases in Greece, between 2005 and 2010, in relation to percent dog seropositivity, *Leishmania* spp., and zymodeme (zymodeme: MON-1, MON-98 *L. infantum*; MON-300, MON-58, MON-57 *L. tropica*). (Key map: Attiki region showing the four prefectures). Only data with more than 60 examined dogs per prefecture were taken into account for the mapping of the results.

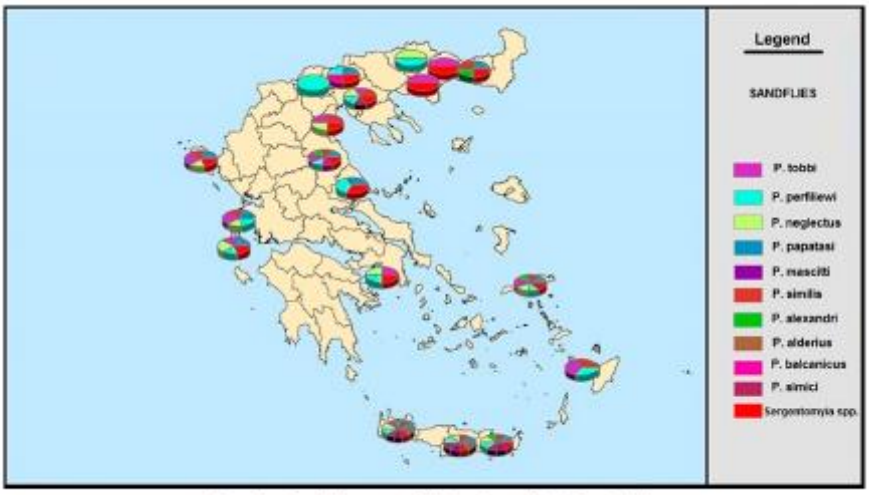

FIGURE 3. Recorded presence of phlebotomine sandflies in Greece.[15–17]

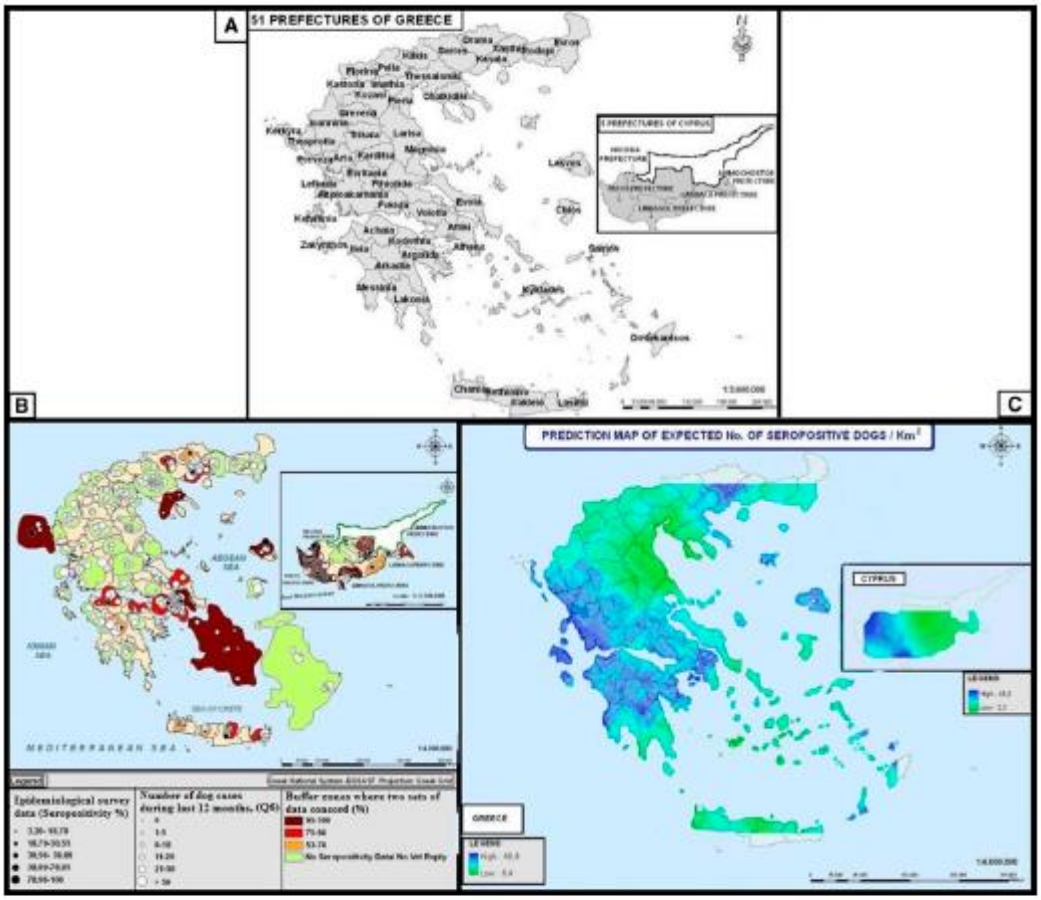

FIGURE 1. (**A**) The study area of Greece and Cyprus showing prefectures. (**B**) Comparison of the two sets of data (dog seropositivity data obtained from two epidemiological surveys[9,10] and the VQ data) on the local level by spatial analysis (GIS software). In the locations where both sets of data were available, the data matched by 53–100%, with the majority showing over 75% concordance. (**C**) Predictive maps of areas at high risk of the spread of CanL prepared with VQ data compared with those maps based on dog seroprevalence data.[9,10]